HYPERBOLIC HEAT CONDUCTION IN COMPOSITE MATERIALS

Wensheng Shen* & Sam Han+
Department of Mechanical Engineering
Tennessee Tech University
Cookeville, TN 38505

Abstract

A hyperbolic heat conduction (HHC) equation has been proposed to replace Fourier heat conduction equation in cases heat transfer takes place in a very short period of time or at extremely low temperature. There is a growing interest in the investigation of HHC problem in recent years, but to the author's knowledge, HHC in composite media in multi-dimension has not been studied up to date. This paper presents a numerical method to solve two-dimensional HHC in composite materials. The numerical method used in the paper is free of oscillation in predicting the solution of hyperbolic systems encountering discontinuities. The key to solve HHC in composite media is to keep both temperature and heat flux continuous at the interfaces. The HHC equation is non-dimensionalized in a way, so that the HHC problem in composite media can be solved in non-dimensional form.

Nomenclature

$[A]$, $[B]$	Jacobian matrix
c	thermal wave speed
C_p	specific Heat
$\mathbf{E}$, $\overline{\mathbf{E}}$	flux vector
$\mathbf{F}$, $\overline{\mathbf{F}}$	flux vector
g	heat source
k	thermal conductivity
q	heat flux
$[R]$, $[R]^{-1}$	matrix
$\mathbf{S}$, $\overline{\mathbf{S}}$	source vector
t	time
T	temperature
Tr	reference temperature
$\mathbf{U}$, $\overline{\mathbf{U}}$	Vector of unknown varibles
W	characteristic variable
$\mathbf{W}$	vector of characteristic variables
x, y	coordinates variables

Greek Symbols

α	thermal diffusivity ($k/(\rho C_p)$)
Δ	variable difference
λ	eigenvalue
ξ, η	coordinates direction
ρ	density
τ	relaxation time (α / c^2)
ψ	limiter function

Superscripts

i	i th characteristic
n	time level n
u	upwind scheme
$*$	non-dimensionlized variable

Subscripts

A , B	matrixes $[A]$ and $[B]$
x , y	coordinates direction
ξ , η	coordinates direction

Introduction

In situations dealing with transient heat transfer in an extremely short period of time and at a temperature near absolute zero, the wave nature of heat propagation can be observed. Peshkov [1] performed one of the earliest experiments to detect thermal waves in liquid helium in 1944. In order to account for the wave phenomenon of heat transportation, a modified heat flux equation was proposed by Vernotte [2] and Cattaneo, [3] instead of Fourier's law of heat conduction. In 1984, thermal shocks were observed reflecting from the liquid-vapor interface in superfluid helium by Torczybski, et al.[4] using a conventional schlieren system. Frankel, et al. [5] gave a theoretical investigation of the observed reflections of thermal waves. They presented a general one-dimensional temperature and heat flux formulation for hyperbolic heat conduction in composite materials, as well as a general solution by using a generalized finite integral transform technique.

Present work studies two-dimensional HHC in composite media using characteristics. The method of characteristics has been used to solve one-dimensional and two-dimensional HHC in homogeneous materials,[6,7] but not

* Graduate Student
\+ Professor, Member AIAA

in composite materials. The governing equation of HHC is first non-dimensionalized by using a reference material. The non-dimensional equations are expressed in vector form and are transformed from the Cartesian coordinates to the body-fitted coordinates (BFC) in order to make calculations in complex geometry. The method of fractional step is employed to split a two-dimensional equation into two independent one-dimensional equations. Roe-Sweby's second order explicit TVD scheme [6] is introduced to solve each of the two one-dimensional equations. The characteristics are used to determine the unknown values, either heat flux or temperature, at the boundaries and interfaces. For simplicity, zeroth order approximation of characteristics is applied.

For the parabolic heat conduction (PHC) in composite materials, the thermal conductivity at the interface can be found as the harmonic mean value of adjacent conductivities. In HHC, however, other than thermal conductivity, there are two more properties, thermal diffusivity and relaxation time; therefore, interfacial properties are difficult to be found. Instead, in this work, temperature and heat flux at the interface are calculated explicitly using characteristics, assuming that both heat flux and temperature are continuous at the interface.

Mathematical Formulation and Analysis

The non-dimensional form of HHC equation has been widely used,[6-13] but none of the physical properties appears in the form. Therefore, non-dimensional HHC equations in that form can't be used directly to investigate the thermal wave phenomena in composite materials. In this section the governing equations of HHC are non-dimensionalized in a way, so that physical properties of different materials can be expressed in non-dimensional equations, in consequence, the HHC in composite materials can be studied in non-dimensional form. The obtained non-dimensional HHC equations are then transformed to the curvilinear coordinates.

Two-dimensional HHC Equations in The x-y Coordinates

The two-dimensional governing equations of HHC in the x-y coordinates are given by

$$-\frac{\partial q_x}{\partial x}-\frac{\partial q_y}{\partial y}+g(x,y,t)=\rho C_p\frac{\partial T}{\partial t} \tag{1a}$$

$$q_x+\tau\frac{\partial q_x}{\partial t}=-k\frac{\partial T}{\partial x} \tag{1b}$$

$$q_y+\tau\frac{\partial q_y}{\partial t}=-k\frac{\partial T}{\partial y} \tag{1c}$$

Assuming a reference material with physical properties of ρ_0, C_{p0}, k_0, and τ_0, the physical properties of other materials are expressed as $\rho=\rho_0\rho^*$, $C_p=C_{p0}C_p^*$, $k=k_0k^*$, and $\tau=\tau_0\tau^*$. Noticing the relationship of $\alpha=k/(\rho C_p)$, it is clear that $\alpha=\alpha_0\alpha^*$.

Substituting the above expressions of physical properties into Eqs. (1a), (1b) and (1c), the following non-dimensional HHC equations can be obtained:

$$\frac{\partial T^*}{\partial t^*}+\frac{\alpha^*}{k^*}\frac{\partial q_x^*}{\partial x^*}+\frac{\alpha^*}{k^*}\frac{\partial q_y^*}{\partial y^*}=\frac{\alpha^*}{k^*}\frac{g^*}{2} \tag{2a}$$

$$\frac{\partial q_x^*}{\partial t^*}+\frac{k^*}{\tau^*}\frac{\partial T^*}{\partial x^*}=-\frac{2q_x^*}{\tau^*} \tag{2b}$$

$$\frac{\partial q_y^*}{\partial t^*}+\frac{k^*}{\tau^*}\frac{\partial T^*}{\partial y^*}=-\frac{2q_y^*}{\tau^*} \tag{2c}$$

where the dimensionless variables are given by

$$q_x^*=\frac{\alpha_0 q_x}{c_0k_0T_r},\quad q_y^*=\frac{\alpha_0 q_y}{c_0k_0T_r},\quad T^*=\frac{T}{T_r},\quad t^*=\frac{c_0^2t}{2\alpha_0},$$

$$x^*=\frac{c_0x}{2\alpha_0},\ y^*=\frac{c_0y}{2\alpha_0},\ g^*=\frac{4\alpha_0^2g}{c_0^2k_0T_r}$$

Assuming the physical properties α, k, and τ are locally constant, Eqs (2a), (2b) and (2c) can be rewritten as

$$\frac{\partial T^*}{\partial t^*}+\frac{\partial(\alpha^*q_x^*/k^*)}{\partial x^*}+\frac{\partial(\alpha^*q_y^*/k^*)}{\partial y^*}=\frac{\alpha^*}{k^*}\frac{g^*}{2} \tag{3a}$$

$$\frac{\partial q_x^*}{\partial t^*}+\frac{\partial(k^*T^*/\tau^*)}{\partial x^*}=-\frac{2q_x^*}{\tau^*} \tag{3b}$$

$$\frac{\partial q_y^*}{\partial t^*}+\frac{\partial(k^*T^*/\tau^*)}{\partial y^*}=-\frac{2q_y^*}{\tau^*} \tag{3c}$$

For simplicity, superscript *'s are omitted hereafter. Rewriting Eqs. (3a), (3b) and (3c) in vector form

$$\frac{\partial\mathbf{U}}{\partial t}+\frac{\partial\mathbf{E}}{\partial x}+\frac{\partial\mathbf{F}}{\partial y}=\mathbf{S} \tag{4}$$

where,

$$\mathbf{U}=[T,q_x,q_y]^T$$

$$\mathbf{E}=[\frac{\alpha}{k}q_x,\frac{k}{\tau}T,0]^T$$

$$\mathbf{F}=[\frac{\alpha}{k}q_y,0,\frac{k}{\tau}T]^T$$

$$\mathbf{S}=[\frac{\alpha}{k}\frac{g}{2},-2\frac{q_x}{\tau},-2\frac{q_y}{\tau}]^T$$

Two-dimensional HHC Equations in The Curvilinear Coordinates

To simplify the implementation of boundary conditions, the domain of interest is transformed from the physical space to the computational space, which is in rectangular shape. The governing equations of HHC in 2-D need to be transformed from the physical coordinates (x, y) to the computational coordinates (ξ, η) as well, such that

calculations are carried out in the computational coordinates rather than in the physical coordinates.

The physical coordinates (x , y) and the computational coordinates (ξ , η) are related by

$$x = x(\xi,\eta)\,,\ y = y(\xi,\eta) \tag{5}$$

Then the governing equations of HHC in the computational coordinates can be found from Eqs. (3a), (3b) and (3c) as

$$\frac{\partial T}{\partial t}+\frac{\partial(\alpha q_x/k)}{\partial \xi}\xi_x+\frac{\partial(\alpha q_x/k)}{\partial \eta}\eta_x + \frac{\partial(\alpha q_y/k)}{\partial \xi}\xi_y+\frac{\partial(\alpha q_y/k)}{\partial \eta}\eta_y=\frac{g}{2}\frac{\alpha}{k} \tag{6a}$$

$$\frac{\partial q_x}{\partial t}+\frac{\partial(kT/\tau)}{\partial \xi}\xi_x+\frac{\partial(kT/\tau)}{\partial \eta}\eta_x=-\frac{2q_x}{\tau} \tag{6b}$$

$$\frac{\partial q_y}{\partial t}+\frac{\partial(kT/\tau)}{\partial \xi}\xi_y+\frac{\partial(kT/\tau)}{\partial \eta}\eta_y=-\frac{2q_y}{\tau} \tag{6c}$$

The metrics in Eqs. (6a), (6b) and (6c) are given by the following expressions:

$$\xi_x = Jy_\eta\,,\ \xi_y = -Jx_\eta\,,\ \eta_x = -Jy_\xi\,,\ \eta_y = -Jx_\xi \tag{7a}$$

where the Jacobian of transformation is given by

$$J = (x_\xi y_\eta - y_\xi x_\eta)^{-1} \tag{7b}$$

Eqs. (6a), (6b) and (6c) can be rewritten as the following vector form:

$$\frac{\partial \overline{\mathbf{U}}}{\partial t}+\frac{\partial \overline{\mathbf{E}}}{\partial \xi}+\frac{\partial \overline{\mathbf{F}}}{\partial \eta}=\overline{\mathbf{S}} \tag{8a}$$

where,

$$\overline{\mathbf{U}}=\frac{1}{J}[T,q_x,q_y]^T$$

$$\overline{\mathbf{E}}=\frac{1}{J}[\xi_x\alpha q_x/k+\xi_y\alpha q_y/k,\xi_x kT/\tau,\xi_y kT/\tau]^T$$

$$\overline{\mathbf{F}}=\frac{1}{J}[\eta_x\alpha q_x/k+\eta_y\alpha q_y/k,\eta_x kT/\tau,\eta_y kT/\tau]^T$$

$$\overline{\mathbf{S}}=\frac{1}{J}[\frac{g}{2}\frac{\alpha}{k},-\frac{2q_x}{\tau},-\frac{2q_y}{\tau}]^T$$

Eq. (8a) can also be written as

$$\frac{\partial \overline{\mathbf{U}}}{\partial t}+[A]\frac{\partial \overline{\mathbf{U}}}{\partial \xi}+[B]\frac{\partial \overline{\mathbf{U}}}{\partial \eta}=\overline{\mathbf{S}} \tag{8b}$$

where, the Jacobian matrix $[A]$ and $[B]$ are respectively

$$[A]=\frac{\partial \overline{\mathbf{E}}}{\partial \overline{\mathbf{U}}}=\begin{pmatrix}0 & \xi_x\dfrac{\alpha}{k} & \xi_y\dfrac{\alpha}{k}\\ \xi_x\dfrac{k}{\tau} & 0 & 0\\ \xi_y\dfrac{k}{\tau} & 0 & 0\end{pmatrix} \tag{9a}$$

$$[B]=\frac{\partial \overline{\mathbf{F}}}{\partial \overline{\mathbf{U}}}=\begin{pmatrix}0 & \eta_x\dfrac{\alpha}{k} & \eta_y\dfrac{\alpha}{k}\\ \eta_x\dfrac{k}{\tau} & 0 & 0\\ \eta_y\dfrac{k}{\tau} & 0 & 0\end{pmatrix} \tag{9b}$$

The matrix $[A]$ in Eq. (8b) may be diagonalized as:

$$[A]=[R_A][\Lambda_A][R_A]^{-1} \tag{10}$$

where $[\Lambda_A]$ is a diagonal matrix, which consists of three eigenvalues of matrix $[A]$. $[R_A]$ is the right eigenmatrix and $[R_A]^{-1}$ is the inverse of matrix $[R_A]$.

The eigenvalues of matrix $[A]$ are

$$\lambda_A^1=0\,,\ \lambda_A^2=\sqrt{\frac{\alpha}{\tau}(\xi_x^2+\xi_y^2)}\,,\ \lambda_A^3=-\sqrt{\frac{\alpha}{\tau}(\xi_x^2+\xi_y^2)} \tag{11a}$$

Therefore the matrixes of $[\Lambda_A]$, $[R_A]$, and $[R_A]^{-1}$ are

$$[\Lambda_A]=\begin{pmatrix}\lambda_A^1 & & \\ & \lambda_A^2 & \\ & & \lambda_A^3\end{pmatrix}=\begin{pmatrix}0 & 0 & 0\\ 0 & \sqrt{\dfrac{\alpha}{\tau}(\xi_x^2+\xi_y^2)} & 0\\ 0 & 0 & -\sqrt{\dfrac{\alpha}{\tau}(\xi_x^2+\xi_y^2)}\end{pmatrix} \tag{11b}$$

$$[R_A]=\begin{pmatrix}0 & 1 & 1\\ \dfrac{-\xi_y}{\sqrt{\frac{\alpha}{\tau}(\xi_x^2+\xi_y^2)}} & \dfrac{\xi_x\frac{k}{\tau}}{\sqrt{\frac{\alpha}{\tau}(\xi_x^2+\xi_y^2)}} & \dfrac{-\xi_x\frac{k}{\tau}}{\sqrt{\frac{\alpha}{\tau}(\xi_x^2+\xi_y^2)}}\\ \dfrac{\xi_x}{\sqrt{\frac{\alpha}{\tau}(\xi_x^2+\xi_y^2)}} & \dfrac{\xi_y\frac{k}{\tau}}{\sqrt{\frac{\alpha}{\tau}(\xi_x^2+\xi_y^2)}} & \dfrac{-\xi_y\frac{k}{\tau}}{\sqrt{\frac{\alpha}{\tau}(\xi_x^2+\xi_y^2)}}\end{pmatrix} \tag{12a}$$

$$[R_A]^{-1}=\begin{pmatrix}0 & \dfrac{-\xi_y\frac{\alpha}{\tau}}{\sqrt{\frac{\alpha}{\tau}(\xi_x^2+\xi_y^2)}} & \dfrac{\xi_x\frac{\alpha}{\tau}}{\sqrt{\frac{\alpha}{\tau}(\xi_x^2+\xi_y^2)}}\\ \frac{1}{2} & \dfrac{\frac{1}{2}\frac{\alpha}{k}\xi_x}{\sqrt{\frac{\alpha}{\tau}(\xi_x^2+\xi_y^2)}} & \dfrac{\frac{1}{2}\frac{\alpha}{k}\xi_y}{\sqrt{\frac{\alpha}{k}(\xi_x^2+\xi_y^2)}}\\ \frac{1}{2} & \dfrac{\frac{-1}{2}\frac{\alpha}{k}\xi_x}{\sqrt{\frac{\alpha}{\tau}(\xi_x^2+\xi_y^2)}} & \dfrac{\frac{-1}{2}\frac{\alpha}{k}\xi_y}{\sqrt{\frac{\alpha}{\tau}(\xi_x^2+\xi_y^2)}}\end{pmatrix} \tag{12b}$$

Similarly, the eigenvalues, the matrix of eigenvalues, the right eigenmatrix and the inverse of the right eigenmatrix of matrix $[B]$ are found to be

$$\lambda_B^1=0\,,\ \lambda_B^2=\sqrt{\frac{\alpha}{\tau}(\eta_x^2+\eta_y^2)}\,,\ \lambda_B^3=-\sqrt{\frac{\alpha}{\tau}(\eta_x^2+\eta_y^2)} \tag{13a}$$

$$[\Lambda_B]=\begin{pmatrix}\lambda_B^1 & & \\ & \lambda_B^2 & \\ & & \lambda_B^3\end{pmatrix}=\begin{pmatrix}0 & 0 & 0\\ 0 & \sqrt{\frac{\alpha}{\tau}(\eta_x^2+\eta_y^2)} & 0\\ 0 & 0 & -\sqrt{\frac{\alpha}{\tau}(\eta_x^2+\eta_y^2)}\end{pmatrix} \quad (13b)$$

$$[R_B]=\begin{pmatrix}0 & 1 & 1\\ \frac{-\eta_y}{\sqrt{\frac{\alpha}{\tau}(\eta_x^2+\eta_y^2)}} & \frac{\eta_x\frac{k}{\tau}}{\sqrt{\frac{\alpha}{\tau}(\eta_x^2+\eta_y^2)}} & \frac{-\eta_x\frac{k}{\tau}}{\sqrt{\frac{\alpha}{\tau}(\eta_x^2+\eta_y^2)}}\\ \frac{\eta_x}{\sqrt{\frac{\alpha}{\tau}(\eta_x^2+\eta_y^2)}} & \frac{\eta_y\frac{k}{\tau}}{\sqrt{\frac{\alpha}{\tau}(\eta_x^2+\eta_y^2)}} & \frac{-\eta_y\frac{k}{\tau}}{\sqrt{\frac{\alpha}{\tau}(\eta_x^2+\eta_y^2)}}\end{pmatrix} \quad (14a)$$

$$[R_B]^{-1}=\begin{pmatrix}0 & \frac{-\eta_y\frac{\alpha}{\tau}}{\sqrt{\frac{\alpha}{\tau}(\eta_x^2+\eta_y^2)}} & \frac{\eta_x\frac{\alpha}{\tau}}{\sqrt{\frac{\alpha}{\tau}(\eta_x^2+\eta_y^2)}}\\ \frac{1}{2} & \frac{1}{2}\frac{\eta_x\frac{\alpha}{k}}{\sqrt{\frac{\alpha}{\tau}(\eta_x^2+\eta_y^2)}} & \frac{1}{2}\frac{\eta_y\frac{\alpha}{k}}{\sqrt{\frac{\alpha}{\tau}(\eta_x^2+\eta_y^2)}}\\ \frac{1}{2} & \frac{-1}{2}\frac{\eta_x\frac{\alpha}{k}}{\sqrt{\frac{\alpha}{\tau}(\eta_x^2+\eta_y^2)}} & \frac{-1}{2}\frac{\eta_y\frac{\alpha}{k}}{\sqrt{\frac{\alpha}{\tau}(\eta_x^2+\eta_y^2)}}\end{pmatrix} \quad (14b)$$

Numerical Method

Numerical Scheme

Roe-Sweby's TVD scheme is used in this work to solve HHC equations in the composites. Detailed description of the scheme can be found in a reference.[16] Here the explicit TVD scheme is extended to two-dimensional problems by the fractional step method. The two-dimensional hyperbolic heat conduction system can then be solved by the following steps:

$$\overline{\mathbf{U}}^*_{j,k}=\overline{\mathbf{U}}^n_{j,k}-\frac{\Delta t}{\Delta\xi}(\overline{\mathbf{E}}^n_{j+\frac{1}{2},k}-\overline{\mathbf{E}}^n_{j-\frac{1}{2},k})+\frac{1}{2}\frac{\Delta t}{\Delta\xi}\overline{\mathbf{S}}^n_{j,k} \quad (15a)$$

$$\overline{\mathbf{U}}^{n+1}_{j,k}=\overline{\mathbf{U}}^*_{j,k}-\frac{\Delta t}{\Delta\eta}(\overline{\mathbf{F}}^*_{j,k+\frac{1}{2}}-\overline{\mathbf{F}}^*_{j,k-\frac{1}{2}})+\frac{1}{2}\frac{\Delta t}{\Delta\eta}\overline{\mathbf{S}}^*_{j,k} \quad (15b)$$

In Eq. (15a) numerical flux $\overline{\mathbf{E}}^n_{j+\frac{1}{2},k}$ is evaluated by

$$\overline{\mathbf{E}}^n_{j+\frac{1}{2},k}=\overline{\mathbf{E}}^u_{j+\frac{1}{2},k}+\sum_{i=1}^{3}R^i_{A,j+\frac{1}{2},k}\frac{\psi^i(r^i_{A,j+\frac{1}{2},k})}{2}\times\left[abs(\lambda^i_{A,j+\frac{1}{2},k})-\frac{\Delta t}{\Delta\xi}(\lambda^i_{A,j+\frac{1}{2},k})^2\right]\mathbf{W}_{j+\frac{1}{2},k} \quad (16a)$$

where $\overline{\mathbf{E}}^u_{j+\frac{1}{2},k}$ is the following numerical flux obtained from the first-order upwind scheme:

$$\overline{\mathbf{E}}^u_{j+\frac{1}{2},k}=\frac{1}{2}(\overline{\mathbf{E}}^n_{j+1,k}+\overline{\mathbf{E}}^n_{j,k})-\frac{1}{2}\sum_{i=1}^{3}R^i_{A,j+\frac{1}{2},k}abs(\lambda^i_{A,j+\frac{1}{2},k})\mathbf{W}_{j+\frac{1}{2},k} \quad (16b)$$

and

$$\mathbf{W}_{j+\frac{1}{2},k}=\mathbf{R}^{-1}_{A,j+\frac{1}{2},k}(\overline{\mathbf{U}}^n_{j+1,k}-\overline{\mathbf{U}}^n_{j,k}) \quad (16c)$$

Similarly, $\overline{\mathbf{F}}^*_{j,k+\frac{1}{2}}$ is given by

$$\overline{\mathbf{F}}^*_{j,k+\frac{1}{2}}=\overline{\mathbf{F}}^u_{j,k+\frac{1}{2}}+\sum_{i=1}^{3}R^i_{B,j,k+\frac{1}{2}}\frac{\psi^i(r^i_{B,j+\frac{1}{2},k})}{2}\times\left[abs(\lambda^i_{B,j,k+\frac{1}{2}})-\frac{\Delta t}{\Delta\eta}(\lambda^i_{B,j,k+\frac{1}{2}})^2\right]\mathbf{W}_{j,k+\frac{1}{2}} \quad (17a)$$

where

$$\overline{\mathbf{F}}^u_{j,k+\frac{1}{2}}=\frac{1}{2}(\overline{\mathbf{F}}^*_{j,k+1}+\overline{\mathbf{F}}^*_{j,k})-\frac{1}{2}\sum_{i=1}^{3}R^i_{B,j,k+\frac{1}{2}}abs(\lambda^i_{B,j,k+\frac{1}{2}})\mathbf{W}_{j,k+\frac{1}{2}} \quad (17b)$$

and

$$\mathbf{W}_{j,k+\frac{1}{2}}=\mathbf{R}^{-1}_{B,j,k+\frac{1}{2}}(\overline{\mathbf{U}}^*_{j,k+1}-\overline{\mathbf{U}}^*_{j,k}) \quad (17c)$$

For more information about the implementation of Roe-Sweby's TVD scheme to two-dimensional HHC equations, and the treatment of boundary conditions, references [14,15] can be used.

Heat Flux and Temperature at Interfaces

Without losing generality, a composite medium consisting of two materials is considered. As shown in Fig. 1, the composite media is made of material 1 and material 2, and an interface exists between the two materials.

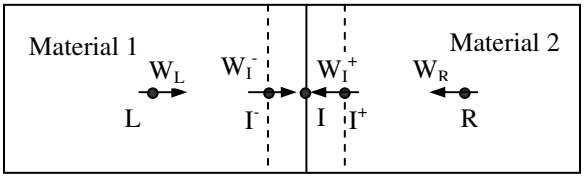

Fig. 1 A two-materials medium and their interface

For simplicity, a one-dimensional case is discussed. It is assumed that there exists a fictitious control volume of zero thickness at the interface. Let the grid point located at the interface be denoted by I, and the corresponding points on the board of the fictitious control volume are I^- and I^+. The nearest grid point to the left of point I is denoted by L, and the nearest grid point to the right of point I is denoted by R. Assuming the physical properties of materials 1 and 2 are constant, and noticing that the information of right running wave at point I comes from point L and that of left running

wave at point I comes from point R, the characteristics at point I^- and I^+ can be determined by Eq. (16c) as

$$W_{I^-} = \frac{1}{2}(T_{I^-} + \frac{\sqrt{\alpha_L \tau_L}}{k_L} q_{I^-}) \tag{18a}$$

and

$$W_{I^+} = \frac{1}{2}(T_{I^+} - \frac{\sqrt{\alpha_R \tau_R}}{k_L} q_{I^+}) \tag{18b}$$

Where W_{I^-} and W_{I^+} can be approximated as

$$W_{I^-} = W_L \text{ and } W_{I^+} = W_R \tag{18c}$$

At the interface of two adjacent regions, a physical condition should be satisfied, i.e., both temperature and heat flux must be continuous.

$$T_I = T_{I^-} = T_{I^+} \tag{19a}$$

and

$$q_I = q_{I^-} = q_{I^+} \tag{19b}$$

Since W_L and W_R have already been known, substituting Eqs. (19a) and (19b) into Eqs (18a) and (18b), and using Eq. (18c), temperature and heat flux at the interface can be found respectively as

$$T_I = \frac{2J_I(\frac{\sqrt{\alpha_R \tau_R}}{k_R} W_L + \frac{\sqrt{\alpha_L \tau_L}}{k_L} W_R)}{\frac{\sqrt{\alpha_L \tau_L}}{k_L} + \frac{\sqrt{\alpha_R \tau_R}}{k_R}} \tag{20a}$$

and

$$q_I = \frac{2J_I(W_L - W_R)}{\frac{\sqrt{\alpha_L \tau_L}}{k_L} + \frac{\sqrt{\alpha_R \tau_R}}{k_R}} \tag{20b}$$

Sample Applications

One-dimension with Two Materials

The simplest problem of HHC in composite medium is that material properties, as well as the temperature distribution, change only in one space direction. Let's Consider HHC in a rectangular cavity with dimensionless size of 1.0×0.1. Assuming the top and bottom boundaries of the rectangular cavity are insulated, the problem becomes one-dimensional. The cavity consists of region 1 and region 2, and each of them is made of a different material. A pulsed volumetric source of width Δx is provided at the left side of region 1 adjacent to $x = 0$. The source can be described as

$$g_1(x,t) = \begin{cases} \dfrac{\delta(t)}{\Delta x}, & 0 < x \le \Delta x \\ 0, & \Delta x < x \le x_1 \end{cases}$$

$$g_2(x,t) = 0, \quad x_1 < x \le x_2 \tag{21}$$

where $\Delta x = 0.05$, $x_1 = 0.5$, and $x_2 = 1$. The left and right boundaries of the cavity are also insulated, and the dimensionless temperature in the cavity is initially 0 everywhere. In the numerical computation, the CFL is 0.5, and 400×40 control volumes are used. For simplicity, we assume the two materials are different only in thermal conductivity with $k_1 = \alpha_1 = \tau_1 = 1$, $\alpha_2 = \tau_2 = 1$, and $k_2 = 2$. Present results are displayed in Figs. 2 and 3, and compared with Frankel, et al.'s one-dimensional solution.[5] Figures 2 and 3 show the temperature distribution and corresponding heat flux distribution respectively at $t = 0.1$ and $t = 0.7$. It is obvious that the numerical solutions agree very well with known analytical solutions.

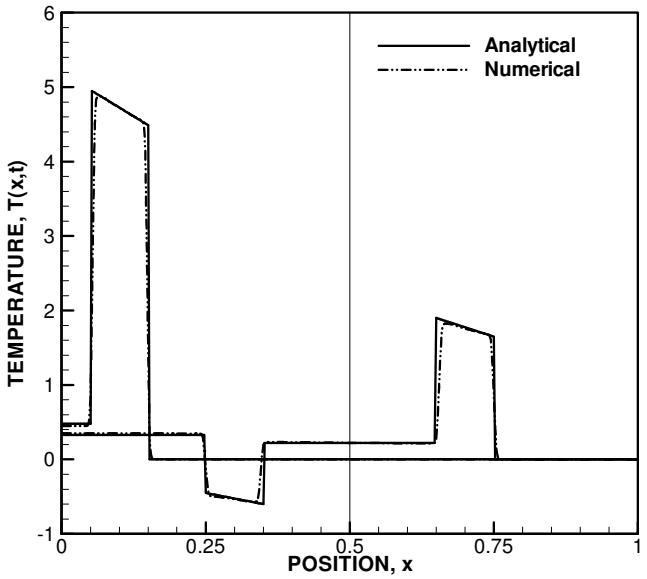

Fig. 2 Comparison of temperature distributions between analytical and numerical solutions at $t = 0.1$ and $t = 0.7$ with $k_1 = 1$ and $k_2 = 2$ (The left half is region 1, and the right half is region 2)

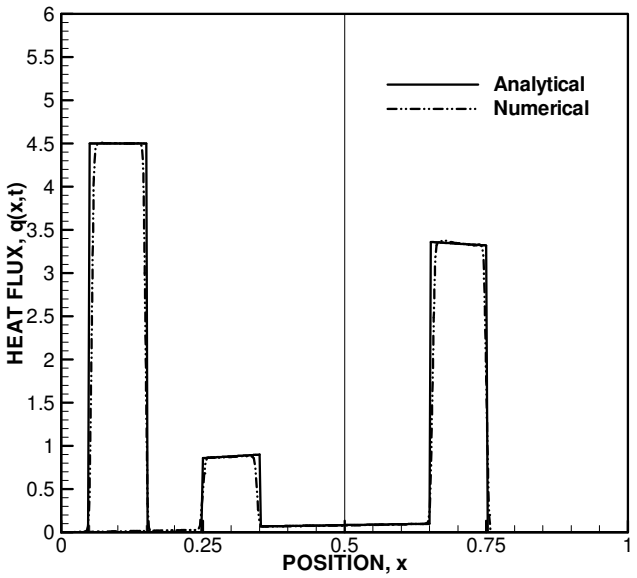

Fig. 3 Comparison of heat flux distributions between analytical and numerical solutions at $t = 0.1$ and $t = 0.7$ with $k_1 = 1$ and $k_2 = 2$ (The left half is region 1, and the right half is region 2)

One-dimension with Three Materials

The same rectangular cavity, boundary conditions, and pulsed volumetric source as those used in the previous examples are applied here. Unlike the previous example, which considered two materials, this example considers three materials. The dimensionless temperature in the cavity is initially 0 everywhere. The source here may be written as

$$g_1(x,t) = \begin{cases} \dfrac{\delta(t)}{\Delta x}, & 0 < x \le \Delta x \\ 0, & \Delta x < x \le x_1 \end{cases}$$

$$g_2(x,t) = 0, \quad x_1 < x \le x_2$$

$$g_3(x,t) = 0, \quad x_2 < x \le x_3 \qquad (22)$$

where $\Delta x = 0.05$, $x_1 = 0.3$, $x_2 = 0.6$, and $x_3 = 1$. In the numerical computation, the CFL is 0.5, and 400×40 control volumes are used.

The influences of k, α, and τ on the thermal wave propagation are studied in this example. Figure 4 shows the effect of k on the temperature distributions at $t = 0.7$ with $k_1 = 1$, $k_2 = 2$, and $k_3 = 0.5$ for solid line, and $k_1 = 1$, $k_2 = 0.5$, and $k_3 = 2$ for dotted-dotted dash line. Constant values are assigned to α and τ. From the mathematical formulation, the wave speed can be express as $c = \lambda_B^2 = \sqrt{\dfrac{\alpha}{\tau}(\eta_x^2 + \eta_y^2)}$ or $c = \lambda_A^2 = \sqrt{\dfrac{\alpha}{\tau}(\xi_x^2 + \xi_y^2)}$, i.e., it is not a function of k. Figure 4 clearly shows that thermal conductivity has no influence on wave speed as well as the pulse width, as we expected. In region 1, the thermal waves are reflected from the left boundary and propagate to the right; in region 2, they are reflected from the interface between regions 2 and 3 and propagate to the left; in region 3, the initial waves propagate to the right with their wave fronts reach at $x = 0.75$.

Figure 5 demonstrates the influence of α to the thermal wave propagation. Since the wave speed is proportional to the square root of α, we expect different speeds in regions 2 and 3. When the thermal diffusivity changes from $\alpha_1 = 1$ to $\alpha_2 = 2$ (solid line), the wave speed increases, and at $t = 0.7$, the thermal wave passes the interface between regions 2 and 3 and propagates in region 3. When the thermal diffusivity changes from $\alpha_1 = 1$ to $\alpha_2 = 0.5$ (dotted -dotted dash line), the wave speed decreases to the extent that the thermal pulse can not pass the interface between region 2 and region 3 completely, and only two pulses can be seen. When α changes from $\alpha_2 = 2$ to $\alpha_3 = 0.5$ (solid line), the wave speed decreases and the width of pulse is decreased too.

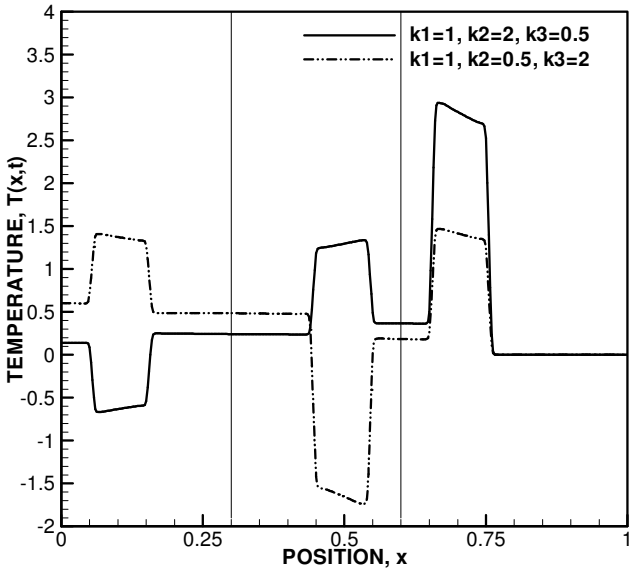

Fig. 4 Effect of k on temperature distributions in composite medium of three regions at $t = 0.7$ (α and τ are kept constant. From the left to the right, regions 1, 2, and 3)

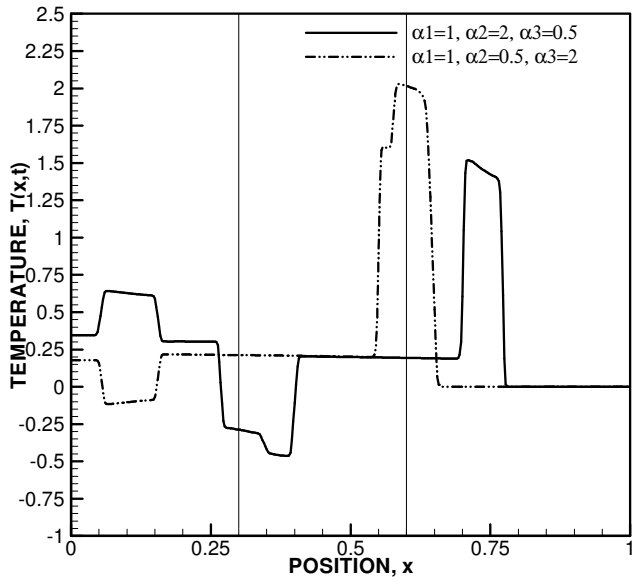

Fig. 5 Effect of α on temperature distributions in composite medium of three regions at $t = 0.7$ (k and τ are kept constant. From the left to the right, regions 1, 2, and 3)

The influence of relaxation time τ to the thermal wave propagation is shown in Fig. 6. The wave speed is affected by proportional to the inverse of the square root of τ. When τ changes from 1 to 2 (solid line), the wave speed decreases, and the initial pulse can not pass the interface of region 2 and region 3 completely at $t = 0.7$. When τ changes from 1 to 0.5 (dotted - dotted dash line), the wave speed increases, and the width of pulse increases as well.

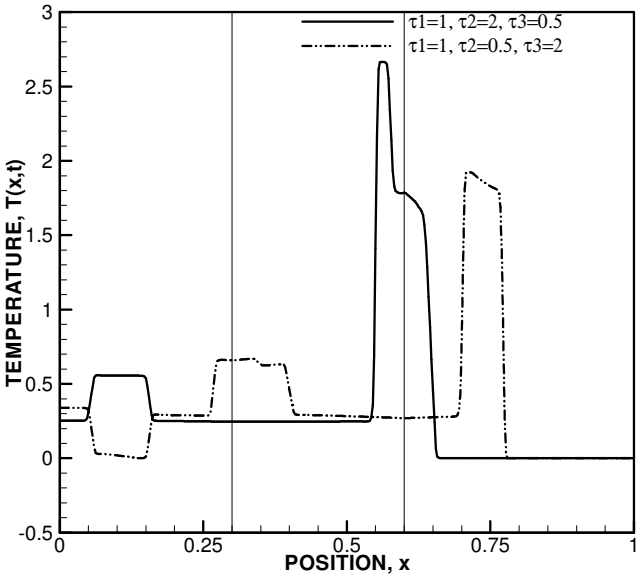

Fig. 6 Effect of τ on temperature distributions in composite medium of three regions at $t = 0.7$ (k and τ are kept constant. From the left to the right, regions 1, 2, and 3)

Two-dimension with Three Materials

In the following space, the results of HHC in composite media in multi-dimension are presented. Without losing generality, we assume a rectangular cavity composed of three materials. The left half of the cavity is made of material 1, and the right half of the cavity is made of materials 2 and 3 respectively, as shown in Fig. 7. For simplicity, the bottom and top walls and the wall at the right-hand side of the cavity are insulated, while a constant temperature of $T = 4$ is maintained at the left-hand side.

Figure 8 shows temperature distributions when all the three regions are made of a single material (material 1). As expected, the temperature distribution is independent of y when three regions have the same material.

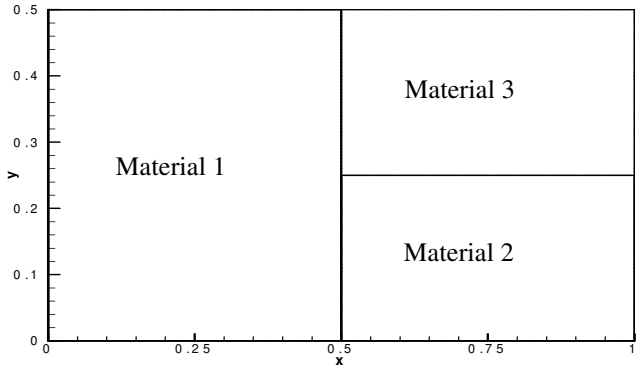

Fig. 7 The domain of two-dimensional calculation

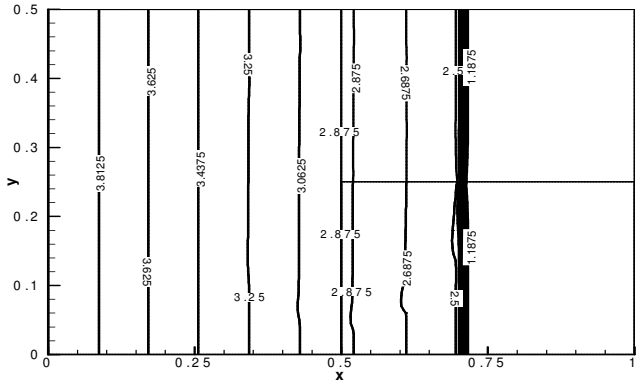

Fig. 8 Temperature distribution with the same material

Figure 9 shows the influences of thermal conductivity k on the thermal wave propagation, and α and τ are kept constant. Comparing Fig. 8 with Fig. 9, it is obvious that k has no influence on the thermal wave speed, but affects the temperature value. Generally speaking, higher k gives lower temperature, i.e., at the same x location, the temperature in region 2 is lower than that in region 3.

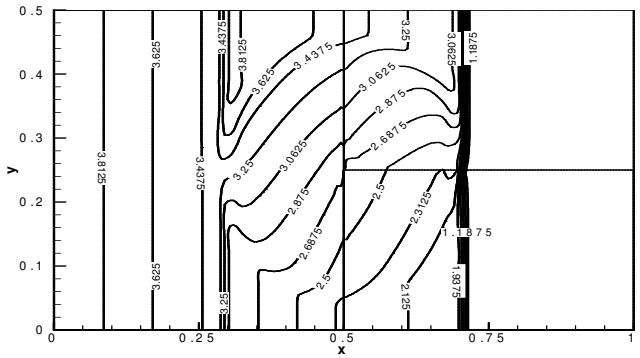

Fig. 9 The influence of k on thermal wave propagation with $k_1 = 1$, $k_2 = 2$, and $k_3 = 0.5$

The influence of thermal diffusivity α on the thermal wave propagation is exhibited in Fig. 10. The values of k and τ are kept constant. As observed in one-dimension situation, larger α (region 2) results in higher thermal wave speed, and smaller α (region 3) results in lower thermal wave speed. The thermal wave in region 2 moves faster than that in region 3. Near the top and bottom boundaries, sharp discontinuities can be seen in the vicinity of the thermal wave fronts. Near the interface between regions 2 and 3, however, no such discontinuities are observed, because of the wave reflection and interaction cased by the difference of α.

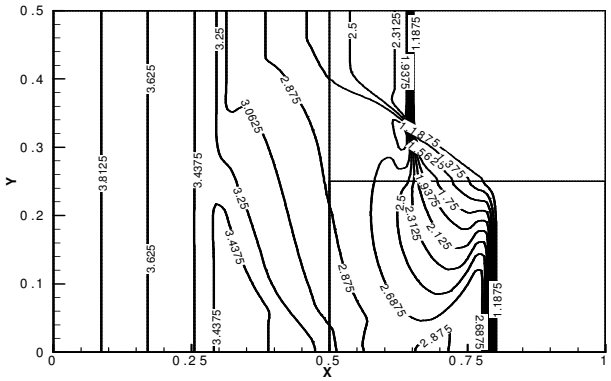

Fig. 10 The influence of α on thermal wave propagation with $\alpha_1 = 1$, $\alpha_2 = 2$, and $\alpha_3 = 0.5$

Figure 11 displays the influence of relaxation time τ on temperature distributions. The values of k and α are the same in all three regions, while τ varies as $\tau_1 = 1$, $\tau_2 = 2$, and $\tau_3 = 0.5$. In region 1, because of the interfaces between regions 1 and 2 and between regions 1 and 3, reflected thermal waves are observed and their fronts propagate to the location at about $x = 0.3$. Temperatures in the front of reflected waves are not affected, while those behind the reflected waves are changed. Unlike in one-dimensional case, the temperature distribution here caused by reflection is a function of both x and y, for τ is different in region 2 and region 3, and the strength of reflected waves is affected by the value of τ too. The thermal wave in region 2 moves slower than that in region 3, because τ is larger in region 2 than that in region 3, as mentioned in one-dimensional situation. The same as that obtained for the influence of α, there is no sharp discontinuities in the vicinity of the thermal wave front near the interface of regions 2 and 3, because of the wave reflection and interaction caused by the difference of τ.

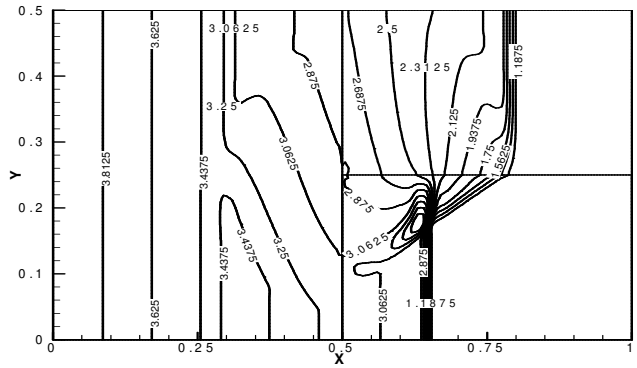

Fig. 11 The influence of τ on thermal wave propagation with $\tau_1 = 1$, $\tau_2 = 2$, and $\tau_3 = 0.5$

Figure 12 demonstrates the influences of combined k, α, and τ on the thermal wave propagation with $k_1 = \alpha_1 = \tau_1 = 1$, $k_2 = \alpha_2 = 2$ and $\tau_2 = 1$, and $k_3 = 2$, $\alpha_3 = 0.5$, and $\tau_3 = 1$. Since here $\tau_1 = \tau_2 = \tau_3 = 1$, thermal wave speed is only affected by α. Since the values of α in regions 2 and 3 in Fig. 12 are the same as those in Fig. 10, thermal waves here in regions 2 and 3 show the same pattern as those in Fig. 10, but different in the reflected part in region 1. The difference comes from thermal conductivity k. Here $k_2 = k_3 = 2$, consequently, the reflected waves in region 1 are stronger and the temperatures in regions 2 and 3 and the reflected part in region 1 are lower than those in Fig. 10.

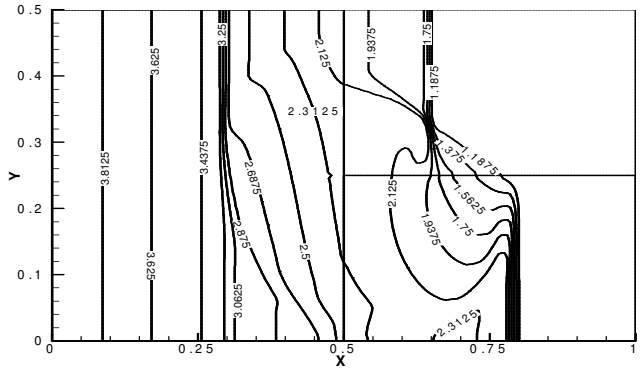

Fig. 12 Influences of combined k, α, and τ on the thermal wave propagation with $k_1 = \alpha_1 = \tau_1 = 1$, $k_2 = \alpha_2 = 2$ and $\tau_2 = 1$, and $k_3 = 2$, $\alpha_3 = 0.5$, and $\tau_3 = 1$

Conclusions

An explicit TVD scheme is used to solve HHC equations in composite media, by using characteristics to handle the interfaces between different materials. The present numerical solution is compared with known analytical solution in one-dimensional applications in the open literature, and they agree very well. The influences of material properties such as thermal conductivity, thermal diffusivity and relaxation time on the thermal wave propagation are investigated numerically for both one-dimensional and two-dimensional applications. Numerical solutions give expected results.

Acknowledgement

The authors wish to thank the Center of Manufacturing Research at Tennessee Technological University for the financial support.

References

1. Peshkov, V., " 'Second Sound' in Helium II," *Journal of Physics, USSR*, Vol. VIII, 1944, p. 381.
2. Vernotte, M.P., 1958, "Les paradoxes de la theorie continue de l'equation de la Chaleur," *Comptes Rendus*, Vol. 246 pp. 3154-3155.
3. Cattaneo (Cattaneo, C., 1958, " A form of heat conduction equation which eliminates the paradox of instantaneous propagation,' *Comptes Rendus*, Vol. 247, pp 431-433)
4. J.R. Torczynski, D. Gerthsen, and T. Roesgen, "Schlieren photography of second-sound shock waves in superfluid helium," *Phys. Fluids*, Vol. 27 1984, pp. 2418-2423.
5. Frankel, J.I, Vick, B., and Őzisik, M.N., 1987, "General formulation and analysis of hyperbolic heat conduction in composite media," *Int. J. Heat Mass Transfer*, Vol. 30, 1987, pp. 1293-1305.
6. Yang, H. Q., "Characteristics-based, high-order accurate and nonoscillatory numerical method for hyperbolic heat conduction," *Numerical Heat Transfer, Part B*, vol. 18, pp. 221-241, 1990.
7. Yang, H. Q., "Solution of two-dimensional hyperbolic heat conduction by high-resolution numerical methods, *Numerical Heat Transfer, Part A*, vol. 21, pp. 333-349, 1992.
8. Baumeister, K. J. and Hamill, T. D., "Hyperbolic heat-conduction equation-a solution for the semi-infinite body problem," *ASME J. of Heat Transfer*, vol. 91, pp. 543-548, 1969.
9. Özisik, M. N. and B. Vick, "Propagation and reflection of thermal wave in a finite medium," *Int. J. of Heat and Mass Transfer*, vol. 27, no. 11, pp. 1845-1854, 1984.
10. Glass, D. E., Özisik, M. N., and B. Vick, "Hyperbolic heat conduction with surface radiation," *Int. J. of Heat and Mass Transfer*, vol. 28, no. 10, pp. 1823-1830, 1985.
11. Chen, H.-T. and Lin, H.-Y., "Study of hyperbolic heat conduction with temperature dependant thermal properties," *ASME J. of Heat Transfer*, vol. 116, pp. 750-753, 1994.
12. Kim, W. S., Hector, Jr., L. G., and Özisik, M. N., "Hyperbolic heat conduction due to axisymmetric continuous or pulsed surface heat sources," *J. of Applied Physics*, vol. 68, no. 11, pp. 5478- 5485.
13. Glass, D. E., Özisik, M. N., and McRae, D. S., "Hyperbolic heat conduction with temperature-dependent thermal conductivity," *J. of Applied Physics*, vol. 59, no. 6, pp. 1861-1865, 1986.
14. Shen, W and Han, S., "An explicit TVD scheme for hyperbolic heat conduction in complex geometry," to be published in *Numerical Heat Transfer B*.
15. Shen, W and Han, S., "Numerical Solution of Two-dimensional Axisymmetric Hyperbolic Heat Conduction," to be published in *Computational Mechanics*.
16. Tannehill, J. C., Anderson, D. A., and Pletcher, R. H., *Computational Fluid Mechanics and Heat Transfer, Taylor & Francis*, Washington, 1997.